

Electron's anomalous magnetic-moment effects on electron-hydrogen elastic collisions in the presence of a circularly polarized laser field

S. Elhandi, S. Taj, and Y. Attaourti*

Laboratoire de Physique des Hautes Energies et d'Astrophysique, Faculté des Sciences Semlalia, Université Cadi Ayyad, Boîte Postale 2390, 40000 Marrakech, Morocco

B. Manaut

Université Sultan Moulay Slimane, Faculté Polydisciplinaire, Laboratoire Interdisciplinaire de Recherche en Sciences et Techniques, Boîte Postale 523, 23000 Béni Mellal, Morocco

L. Oufni

Université Sultan Moulay Slimane, Faculté des Sciences et Techniques, Département de Physique, LPMM-ERM, Boîte Postale 523, 23000 Béni Mellal, Morocco

(Received 23 February 2010; published 29 April 2010)

The effect of the electron's anomalous magnetic moment on the relativistic electronic dressing for the process of electron-hydrogen atom elastic collisions is investigated. We consider a laser field with circular polarization and various electric field strengths. The Dirac-Volkov states taking into account this anomaly are used to describe the process in the first order of perturbation theory. The correlation between the terms coming from this anomaly and the electric field strength gives rise to the strong dependence of the spinor part of the differential cross section (DCS) with respect to these terms. A detailed study has been devoted to the nonrelativistic regime as well as the moderate relativistic regime. Some aspects of this dependence as well as the dynamical behavior of the DCS in the relativistic regime have been addressed.

DOI: [10.1103/PhysRevA.81.043422](https://doi.org/10.1103/PhysRevA.81.043422)

PACS number(s): 34.80.Qb, 34.50.Rk, 34.50.Fa, 12.20.Ds

I. INTRODUCTION

The value of the electron's magnetic moment is a fundamental quantity in physics. Its deviation from the value expected from Dirac theory has given enormous impetus to the field of quantum theory and especially to quantum electrodynamics (QED). It is usually expressed in term of the g factor (e.g., for the electron, $g = 2$). This result differs from the observed value by a small fraction of a percent. The difference is the well-known anomalous magnetic moment, denoted a and defined as $a = (g - 2)/2$. The one-loop contribution to the anomalous magnetic moment of the electron is found by calculating the vertex function. The calculation is relatively straightforward [1] and the one-loop result is

$$a = \frac{\alpha}{2\pi} \simeq 0.0011614,$$

where α is the fine structure constant. This result was first found by Schwinger [2] in 1948. A recent experimental value for a was obtained by Gabrielse [3]:

$$a = 0.001159652180(73).$$

The state-of-the-art status of QED predictions of the electron anomaly has been remarkably reviewed by E. Remiddi [4]. As for laser-assisted processes in relativistic atomic physics, the expectation of major advances in laser capabilities has placed a new focus on the fundamentals of QED, which occupies a place of paramount importance among the theories used in the formalism needed to obtain theoretical predictions for the intricate understanding of various fundamental processes. QED has proven itself to be capable of remarkable

quantitative agreement between theoretical predictions and precise laboratory measurements. When presently achievable intensities are around 10^{22} W/cm², electrons are so shaken that their velocity approaches the speed of light. Therefore, the interactions between laser and matter become relativistic. Recently, relativistic laser-atom physics emerged as a new fertile research area. This is due to the newly opened possibility of submitting atoms to ultra-intense pulses of infrared coherent radiation from lasers of various types. The dynamics of a free electron embedded within a constant-amplitude classical field has been addressed since the early years of quantum mechanics. In 1935, an exact expression for the wave function was derived within the framework of the Dirac theory [5]; see also [6] for an overview of the case of an electron submitted to a short laser pulse. In the 1960s, the advent of laser devices motivated theoretical studies related to QED in strong fields. These formal results were considered as being only of academic interest for many years. The state of affairs significantly changed in the mid-1990s when it became possible to collide a relativistic electron beam from a linear accelerator with focused laser (Nd:YAG) radiation. Under such extreme conditions, it has been possible to evidence highly nonlinear essentially relativistic QED processes such as a nonlinear Thomson and Compton scattering and also pair production [7–11]. A first focus issue in 1998 devoted to relativistic effects in strong fields appeared in *Optics Express* [12] and, in 2008, *Strong Field Laser Physics* [13] gave the main advances in this field as well as the references to the works of all major contributors. A seminal thesis [14] addressed the study of laser-assisted second-order relativistic QED processes for the first time. This, we think, will pave the way for a more accurate description of laser-assisted fundamental processes [15,16]. Our aim in this paper is to shed

*attaourti@ucam.ac.ma

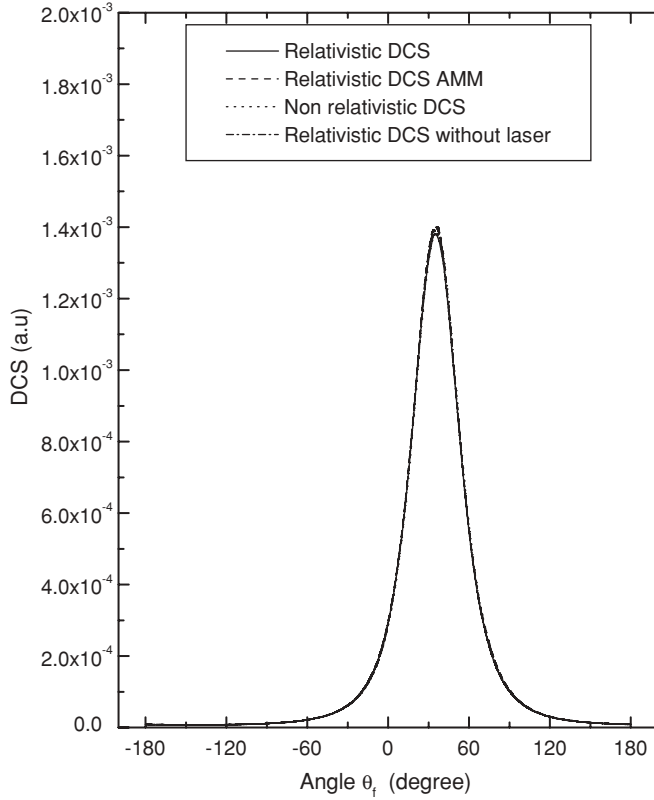


FIG. 1. The various DCSs as a function of the angle θ_f in degrees for an electrical field strength of $\varepsilon = 0.05$ a.u. and a relativistic parameter $\gamma = 1.0053$. The corresponding number of photons exchanged is ± 1200 .

some light on a difficult and recently addressed description of laser-assisted processes that incorporate the electron anomaly. The process under study is the laser-assisted elastic collision of a Dirac-Volkov electron with a hydrogen atom. We focus on the relativistic electronic dressing with the addition of the electron anomaly. Some results are rather surprising, bearing in mind the small value of a . In Sec. II, we present the formalism as well as the coefficients that intervene in the expression of the DCS. In Sec. III, we discuss the results we have obtained in the nonrelativistic, moderate relativistic, and relativistic regimes. Atomic units are used throughout ($\hbar = e = m = 1$), where m denotes the electron mass and work with the metric tensor $g^{\mu\nu} = \text{diag}(1, -1, -1, -1)$.

II. THEORY

The second-order Dirac equation for an electron with anomalous magnetic moment (AMM) in the presence of an external electromagnetic field is [17]

$$\left[\left(p - \frac{1}{c} A \right)^2 - c^2 - \frac{i}{2c} F_{\mu\nu} \sigma^{\mu\nu} + ia \left(\not{p} - \frac{\not{A}}{c} + c \right) F_{\mu\nu} \sigma^{\mu\nu} \right] \times \psi(x) = 0, \quad (1)$$

where $\sigma^{\mu\nu} = \frac{1}{2}[\gamma^\mu, \gamma^\nu]$, γ^μ are the Dirac matrices and $F_{\mu\nu} = \partial_\mu A_\nu - \partial_\nu A_\mu$ is the electromagnetic field tensor. A^μ is the four-vector potential, while $a = \kappa/4$, where κ is the electron's anomaly. The Feynman slash notation is used throughout: $\not{p} =$

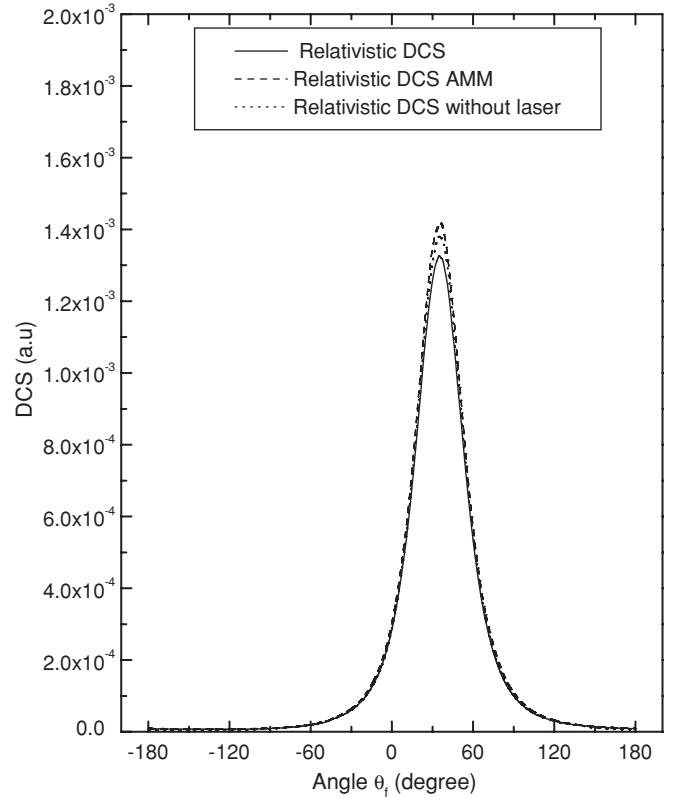


FIG. 2. The various relativistic DCSs as a function of the angle θ_f in degrees for an electrical field strength of $\varepsilon = 0.1$ a.u. and a relativistic parameter $\gamma = 1.0053$. The corresponding number of photons exchanged is ± 1200 .

$p_0\gamma^0 - \mathbf{p}\gamma$ and $\not{A} = A_0\gamma^0 - \mathbf{A}\gamma$. The term $F_{\mu\nu}\sigma^{\mu\nu}$ stems from the fact that the electron has a spin-one-half, and the term multiplying a is due to its AMM. It is possible to rewrite the exact solution found by Y. I. Salamin [18] as

$$\begin{aligned} \psi(x) &= \exp[-(\alpha\not{k}\not{A} + \beta\not{k} + \delta\not{p}\not{k}\not{A})] \frac{u(p,s)}{\sqrt{2VQ_0}} \\ &\times \exp \left\{ -i(px) + i \int_0^{kx} \left[\frac{A^2}{2c^2(kp)} - \frac{(Ap)}{c(kp)} \right] d\phi \right\} \\ &= \exp[-(\alpha\not{k}\not{A} + \beta\not{k} + \delta\not{p}\not{k}\not{A})] \frac{u(p,s)}{\sqrt{2VQ_0}} \\ &\times \exp \left[-i(qx) - i \int_0^{kx} \frac{(Ap)}{c(kp)} d\phi \right], \quad (2) \end{aligned}$$

where

$$\alpha = \frac{ac}{(kp)} - \frac{1}{2c(kp)}, \quad (3)$$

$$\beta = a \frac{A^2}{c(kp)}, \quad (4)$$

$$\delta = \frac{a}{(kp)}. \quad (5)$$

In the preceding equation, the four-vector q^μ is given by

$$q^\mu = p^\mu - \frac{A^2}{2c^2(kp)} k^\mu. \quad (6)$$

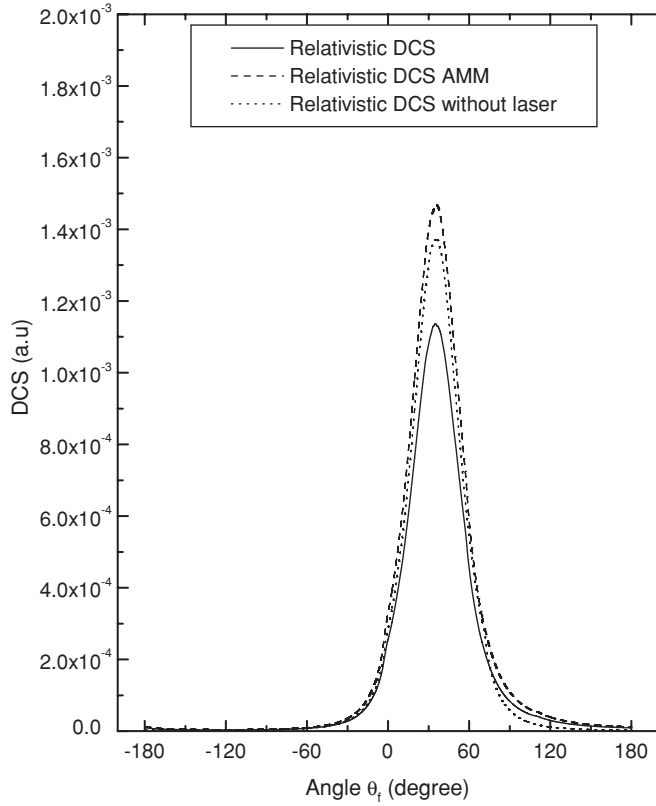


FIG. 3. The various relativistic DCSs as a function of the angle θ_f in degrees for an electrical field strength of $\varepsilon = 0.2$ a.u. and a relativistic parameter $\gamma = 1.0053$. The corresponding number of photons exchanged is ± 1200 .

The four-vector $k^\mu = (\frac{\omega}{c}, \mathbf{k})$ is the four-vector of the circularly polarized laser field $A^\mu = a_1^\mu \cos \phi + a_2^\mu \sin \phi$, $\phi = kx$. Note that k^μ is such that $k^2 = 0$ and $k_\mu A^\mu = 0$, implying that we are working in the Lorentz gauge. One has

$$q^\mu q_\mu = \frac{Q^2}{c^2} - \mathbf{q}^2 = \left(1 - \frac{\overline{A^2}}{c^4}\right) c^2 = m^{*2} c^2, \quad (7)$$

where m^* is the effective mass that the electron acquires when embedded within a laser field:

$$m^* = \left(1 - \frac{\overline{A^2}}{c^4}\right)^{\frac{1}{2}}, \quad (8)$$

We consider laser intensities such that the resulting ponderomotive force is comparable to its rest mass. It is then possible to retain only terms of order 1 in the expansion of the first exponential in Eq. (2) and find

$$\psi(x) = [1 - (\alpha \mathbf{k} \cdot \mathbf{A} + \beta \mathbf{k} + \delta \mathbf{p} \cdot \mathbf{k} \cdot \mathbf{A})] \frac{u(p, s)}{\sqrt{2VQ_0}} \times \exp \left[-i(qx) - i \int_0^{kx} \frac{(Ap)}{c(kp)} d\phi \right]. \quad (9)$$

This expression differs formally from that found by various authors [19] but is actually equivalent. The transition matrix element corresponding to the process of laser assisted electron-atomic hydrogen from the initial state i to the final state f is

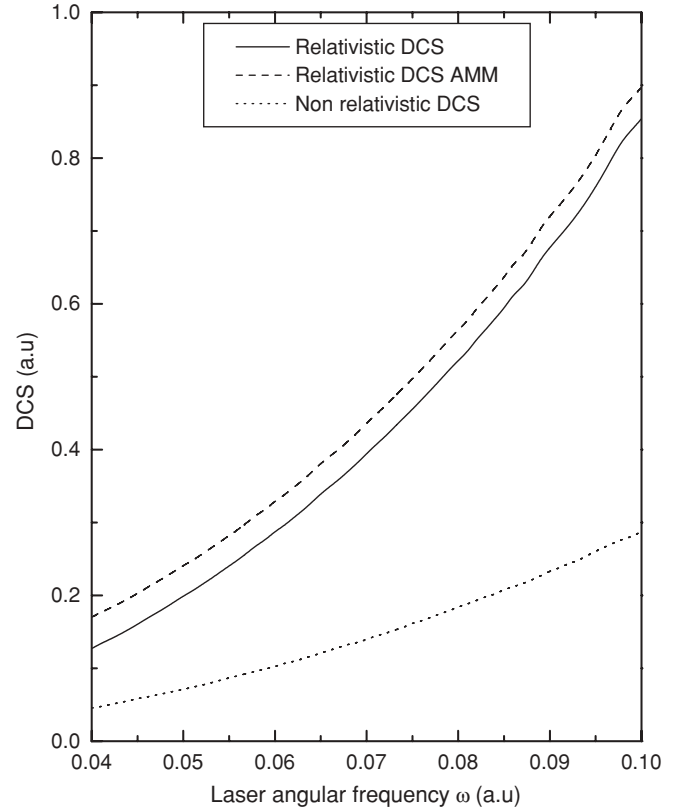


FIG. 4. The various relativistic DCSs scaled in 10^{-5} as a function of ω for an electrical field strength of $\varepsilon = 0.2$ a.u., a relativistic parameter $\gamma = 1.0053$, and an angle $\theta_f = 135^\circ$. The corresponding number of photons exchanged is ± 100 .

given by

$$S_{fi} = -i \int dt \langle \psi_{p_f}(x_1) \phi_f(x_2) | V_d | \psi_{p_i}(x_1) \phi_i(x_2) \rangle. \quad (10)$$

The explicit expression of the wave function of the hydrogen atom $\phi(x_2)$ for the fundamental state (spin up) can be found in [20] and reads

$$\phi(x_2) = \frac{1}{\sqrt{4\pi}} \begin{Bmatrix} ig(x_2) \\ 0 \\ f(x_2) \cos \theta \\ f(x_2) \sin \theta e^{i\phi} \end{Bmatrix}, \quad (11)$$

where $g(x_2)$ is given by

$$g(x_2) = (2Z)^{\gamma+\frac{1}{2}} \sqrt{\frac{1+\gamma}{2\Gamma(1+2\gamma)}} e^{-Zx_2} x_2^{\gamma-1} = N_g e^{-Zx_2} x_2^{\gamma-1} \quad (12)$$

and

$$f(x_2) = -(2Z)^{\gamma+\frac{1}{2}} \sqrt{\frac{1+\gamma}{2\Gamma(1+2\gamma)}} e^{-Zx_2} x_2^{\gamma-1} \frac{(1-\gamma)}{Z\alpha} = N_f e^{-Zx_2} x_2^{\gamma-1}. \quad (13)$$

The instantaneous interaction potential V_d is given by

$$V_d = \frac{1}{x_{12}} - \frac{Z}{x_1}, \quad (14)$$

where $\mathbf{x}_{12} = |\mathbf{x}_1 - \mathbf{x}_2|$; \mathbf{x}_1 are the electron coordinates and \mathbf{x}_2 are the atomic electron coordinates. If we replace all wave functions in Eq. (10), the transition matrix element S_{fi} becomes

$$S_{fi} = -i \sum_{n=-\infty}^{+\infty} \frac{2\pi\delta(Q_f - Q_i - n\omega)}{2V\sqrt{Q_i Q_f}} \times H(\Delta_n) |\bar{u}(p_f, s_f) \Gamma_n u(p_i, s_i)|, \quad (15)$$

where the expression of $H(\Delta_n)$ has already been derived in a previous work [21], and $\Delta_n = |\mathbf{q}_f - \mathbf{q}_i - n\mathbf{k}|$ is the momentum transfer with the net exchange of n photons. We have obtained for $H(\Delta_n)$ the following analytical expression:

$$H(\Delta_n) = -4\pi(N_g^2 + N_f^2)\Gamma(2\gamma + 1) \times \left[\frac{1}{(2Z)^{2\gamma+1}\Delta_n^2} - \frac{\sin(2\gamma\phi)}{2\gamma\lambda^{2\gamma}\Delta_n^3} \right] \quad (16)$$

$$C_0 = [2(2\phi_1 k \phi_i (a_1 p_f) \delta_f \delta_i \omega - 2\phi_1 k \phi_f (a_1 p_i) \delta_f \delta_i \omega + 2\phi_1 k \gamma_0 (a_1 p_i) (k p_f) c \delta_f \delta_i - 2\phi_1 k \gamma_0 (a_1 p_f) (k p_i) c \delta_f \delta_i - 2\phi_1 k (a_1 p_i) \alpha_f \delta_i \omega + 2\phi_1 k (a_1 p_f) \alpha_i \delta_f \omega + 2\phi_2 k \phi_i (a_2 p_f) \delta_f \delta_i \omega - 2\phi_2 k \phi_f (a_2 p_i) \delta_f \delta_i \omega + 2\phi_2 k \gamma_0 (a_2 p_i) (k p_f) c \delta_f \delta_i - 2\phi_2 k \gamma_0 (a_2 p_f) (k p_i) c \delta_f \delta_i - 2\phi_2 k (a_2 p_i) \alpha_f \delta_i \omega + 2\phi_2 k (a_2 p_f) \alpha_i \delta_f \omega - 2k \phi_i \alpha_f A^2 \delta_i \omega + 2k \phi_f \alpha_i A^2 \delta_f \omega - 2k \phi_f \gamma_0 (k p_i) A^2 c \delta_f \delta_i + 2k \phi_f \alpha_i A^2 \delta_f \omega - 2k \gamma_0 \phi_i (k p_f) A^2 c \delta_f \delta_i + 2k \gamma_0 (k p_i) \alpha_f A^2 c \delta_i - 2k \gamma_0 (k p_f) \alpha_i A^2 c \delta_f - k \gamma_0 \beta_f c - 2k \alpha_f \alpha_i A^2 \omega + 2k \beta_f \beta_i \omega - \gamma_0 k \beta_i c + \gamma_0 c)] / (2c) \quad (19)$$

$$C_1 = [2(-\phi_1 k \phi_f \gamma_0 c \delta_f + 2\phi_1 k \phi_f \beta_i \delta_f \omega - 2\phi_1 k \gamma_0 (k p_f) \beta_i c \delta_f - \phi_1 k \gamma_0 \alpha_f c + 2\phi_1 k \alpha_f \beta_i \omega + 2k \phi_1 \alpha_i \beta_f \omega - 2k \phi_i \phi_1 \beta_f \delta_i \omega + 2k \gamma_0 \phi_1 (k p_i) \beta_f c \delta_i - \gamma_0 k \phi_1 \alpha_i c - \gamma_0 \phi_i k \phi_1 c \delta_i)] / (2c) \quad (20)$$

$$C_2 = [2(-\phi_2 k \phi_f \gamma_0 c \delta_f + 2\phi_2 k \phi_f \beta_i \delta_f \omega - 2\phi_2 k \gamma_0 (k p_f) \beta_i c \delta_f - \phi_2 k \gamma_0 \alpha_f c + 2\phi_2 k \alpha_f \beta_i \omega + 2k \phi_2 \alpha_i \beta_f \omega - 2k \phi_i \phi_2 \beta_f \delta_i \omega + 2k \gamma_0 \phi_2 (k p_i) \beta_f c \delta_i - \gamma_0 k \phi_2 \alpha_i c - \gamma_0 \phi_i k \phi_2 c \delta_i)] / (2c) \quad (21)$$

$$C_3 = [4(\phi_1 k \phi_i (a_1 p_f) \delta_f \delta_i \omega - \phi_1 k \phi_f (a_1 p_i) \delta_f \delta_i \omega + \phi_1 k \gamma_0 (a_1 p_i) (k p_f) c \delta_f \delta_i - \phi_1 k \gamma_0 (a_1 p_f) (k p_i) c \delta_f \delta_i - \phi_1 k (a_1 p_i) \alpha_f \delta_i \omega + \phi_1 k (a_1 p_f) \alpha_i \delta_f \omega - \phi_2 k \phi_i (a_2 p_f) \delta_f \delta_i \omega + \phi_2 k \phi_f (a_2 p_i) \delta_f \delta_i \omega - \phi_2 k \gamma_0 (a_2 p_i) (k p_f) c \delta_f \delta_i + \phi_2 k \gamma_0 (a_2 p_f) (k p_i) c \delta_f \delta_i + \phi_2 k (a_2 p_i) \alpha_f \delta_i \omega - \phi_2 k (a_2 p_f) \alpha_i \delta_f \omega)] / (2c) \quad (22)$$

$$C_4 = [4(\phi_1 k \phi_i (a_2 p_f) \delta_f \delta_i \omega - \phi_1 k \phi_f (a_2 p_i) \delta_f \delta_i \omega + \phi_1 k \gamma_0 (a_2 p_i) (k p_f) c \delta_f \delta_i - \phi_1 k \gamma_0 (a_2 p_f) (k p_i) c \delta_f \delta_i - \phi_1 k (a_2 p_i) \alpha_f \delta_i \omega + \phi_1 k (a_2 p_f) \alpha_i \delta_f \omega + \phi_2 k \phi_i (a_1 p_f) \delta_f \delta_i \omega - \phi_2 k \phi_f (a_1 p_i) \delta_f \delta_i \omega + \phi_2 k \gamma_0 (a_1 p_i) (k p_f) c \delta_f \delta_i - \phi_2 k \gamma_0 (a_1 p_f) (k p_i) c \delta_f \delta_i - \phi_2 k (a_1 p_i) \alpha_f \delta_i \omega + \phi_2 k (a_1 p_f) \alpha_i \delta_f \omega)] / (2c) \quad (23)$$

The coefficients C_i contain all the information about the effect of the electron's AMM since they depend on $\kappa = 4a$. Therefore, it is to be expected that this aforementioned effect should be of crucial importance since both κ and the electric field strength are correlated in the expression of the five coefficients C_i . We now introduce the well-known relations involving ordinary Bessel functions:

$$\begin{Bmatrix} 1 \\ \cos(\phi) \\ \sin(\phi) \\ \cos(2\phi) \\ \sin(2\phi) \end{Bmatrix} e^{-iz \sin(\phi - \phi_0)} = \sum_{n=-\infty}^{\infty} \begin{Bmatrix} B_{0n} \\ B_{1n} \\ B_{2n} \\ B_{3n} \\ B_{4n} \end{Bmatrix} e^{-in\phi}, \quad (24)$$

with

$$\lambda = \sqrt{(2Z)^2 + \Delta_n^2} \quad \text{and} \quad \phi = \arctan\left(\frac{\Delta_n}{2Z}\right). \quad (17)$$

However, the novelty in the various stages of the calculations is contained in the term $|\bar{u}(p_f, s_f) \Gamma_n u(p_i, s_i)|$, where

$$\begin{aligned} \Gamma_n &= \bar{R}(p_f) \gamma^0 R(p_i) \\ &= [1 - (\alpha_f \not{A} \not{k} + \beta_f \not{k} + \delta_f \not{A} \not{k} \not{p}_f)] \gamma^0 \\ &\quad \times [1 - (\alpha_i \not{k} \not{A} + \beta_i \not{k} + \delta_i \not{p}_i \not{k} \not{A})] \\ &= C_0 + C_1 \cos \phi + C_2 \sin \phi + C_3 \cos 2\phi + C_4 \sin 2\phi. \end{aligned} \quad (18)$$

These coefficients can be obtained using REDUCE [22]. We give their analytical expressions:

with

$$\begin{Bmatrix} B_{0n} \\ B_{1n} \\ B_{2n} \\ B_{3n} \\ B_{4n} \end{Bmatrix} = \begin{Bmatrix} J_n(z) e^{in\phi_0} \\ (J_{n+1}(z) e^{i(n+1)\phi_0} + J_{n-1}(z) e^{i(n-1)\phi_0}) / 2 \\ (J_{n+1}(z) e^{i(n+1)\phi_0} - J_{n-1}(z) e^{i(n-1)\phi_0}) / 2i \\ (J_{n+2}(z) e^{i(n+2)\phi_0} + J_{n-2}(z) e^{i(n-2)\phi_0}) / 2 \\ (J_{n+2}(z) e^{i(n+2)\phi_0} - J_{n-2}(z) e^{i(n-2)\phi_0}) / 2i \end{Bmatrix}. \quad (25)$$

The product of the terms given by Eq. (18) can be written as

$$\Gamma_n = \sum_{n=-\infty}^{+\infty} (C_0 B_{0n} + C_1 B_{1n} + C_2 B_{2n} + C_3 B_{3n} + C_4 B_{4n}). \quad (26)$$

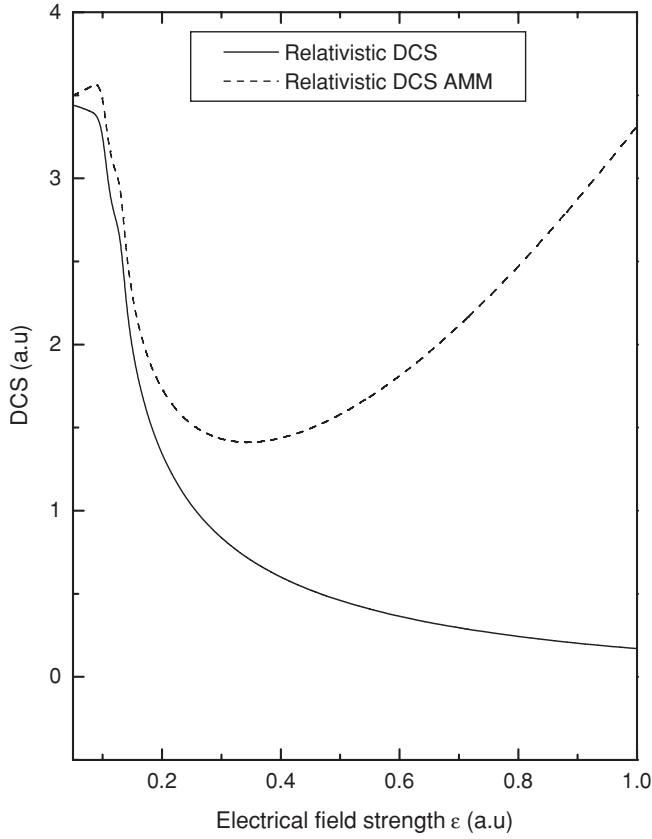


FIG. 5. The two interesting DCSs scaled in 10^{-5} as a function of electrical field strength of ε for a relativistic parameter $\gamma = 1.0053$ and an angle $\theta_f = 135^\circ$. The corresponding number of photons exchanged is ± 1000 .

Proceeding along the lines of standard QED calculations [8], for the formal differential cross section (DCS) expression in the presence of a circularly polarized laser field and taking into account the AMM of the electron, we obtain

$$\left. \frac{d\sigma}{d\Omega_f} \right|_{Q_f=Q_i+n\omega} = \sum_{n=-\infty}^{\infty} \frac{1}{(4\pi c^2)^2} \frac{|\mathbf{q}_f|}{|\mathbf{q}_i|} \frac{1}{2} \sum_{s_i} \sum_{s_f} |M_{fi}^{(n)}|^2 |H(\Delta_n)|^2 \Big|_{Q_f=Q_i+n\omega}, \quad (27)$$

where

$$\frac{1}{2} \sum_{s_i} \sum_{s_f} |M_{fi}^{(n)}|^2 = \frac{1}{2} \text{Tr}[(\not{p}_f c + c^2)\Gamma_n(\not{p}_i c + c^2)\bar{\Gamma}_n], \quad (28)$$

$$\bar{\Gamma}_n = \gamma^0 \Gamma_n^\dagger \gamma^0. \quad (29)$$

III. RESULTS AND DISCUSSION

The geometry chosen is $\theta_i = \phi_i = 45^\circ$ for the incident electron, while for the scattered electron $\phi_f = 90^\circ$ and the angle θ_f varies from -180° to 180° . For all the angular distributions of the DCSs, we maintain the same choice of the laser angular frequency, that is, $\omega = 0.0043$ a.u., which corresponds to a near-infrared neodymium laser. Also, for the

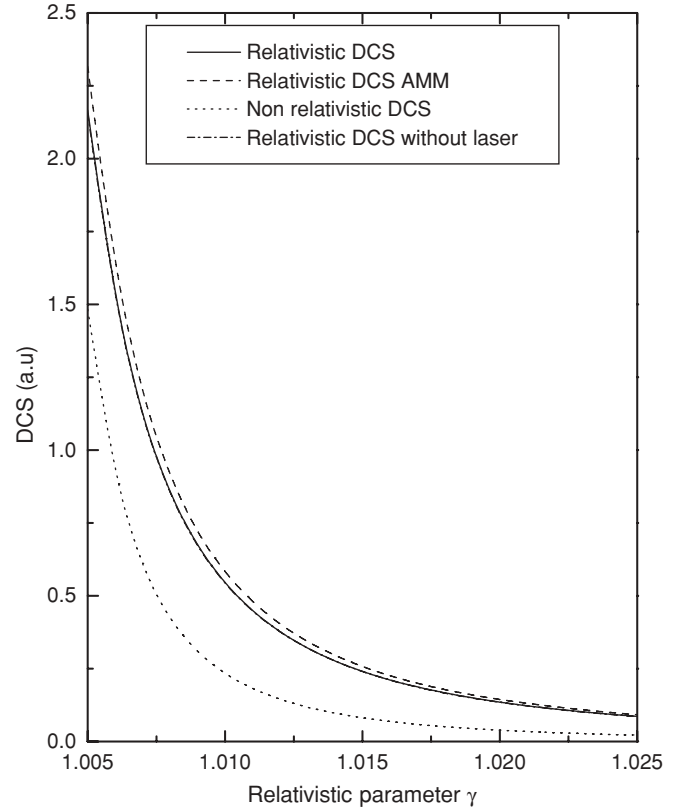


FIG. 6. Various DCSs scaled in 10^{-5} as a function of relativistic parameter γ for an electrical field strength of $\varepsilon = 0.1$ a.u. and an angle $\theta_f = 135^\circ$. The corresponding number of photons exchanged is ± 1000 .

investigation of the behavior of the various DCSs with respect to the electric field strength ε and the relativistic parameter γ , ω is fixed at the same value. The dependence of the DCSs with respect to the laser frequency is investigated, beginning with frequencies $\omega_{\min} = 0.04$ a.u. to $\omega_{\max} = 0.1$ a.u.

We define some useful abbreviations that simplify the readability of the text: $(d\sigma/d\Omega_f)^{RNL}$ denotes relativistic DCS without a laser field while $(d\sigma/d\Omega_f)^{RL}$ denotes relativistic DCS with a laser field; $(d\sigma/d\Omega_f)^{NRL}$ is the nonrelativistic DCS with a laser field and $(d\sigma/d\Omega_f)^{RL}_{AMM}$ is DCS with AMM in the presence of a laser field.

A. The nonrelativistic regime

For an electron with a low kinetic energy and a moderate field strength, typically $E_c = 100$ a.u. (or $E_c = 2700$ eV) and a field strength $\varepsilon = 0.05$ a.u., the nondressed momentum coordinates $(\mathbf{p}_i, \mathbf{p}_f)$ and $(\mathbf{q}_i, \mathbf{q}_f)$ are relatively close. We have carried out numerical simulations for $\varepsilon = 0.05$ a.u. and $\gamma = 1.0053$. Since the DCSs are sensitive to the number n of photons exchanged, we have used $(d\sigma/d\Omega_f)^{RNL}$ as a reference to see how the others evolve with increasing values of n . For $n = \pm 100$ photons, the figure obtained is not physically sound since it is nonrelativistic; $(d\sigma/d\Omega_f)^{RL}$ and $(d\sigma/d\Omega_f)^{RL}_{AMM}$ are close, but a small difference appears at the peaks located near $\theta_f = 33^\circ$. In other words, n must be increased. For $n = \pm 400$ photons, a newly found result (as far as we know) is the violation of the pseudo-sum

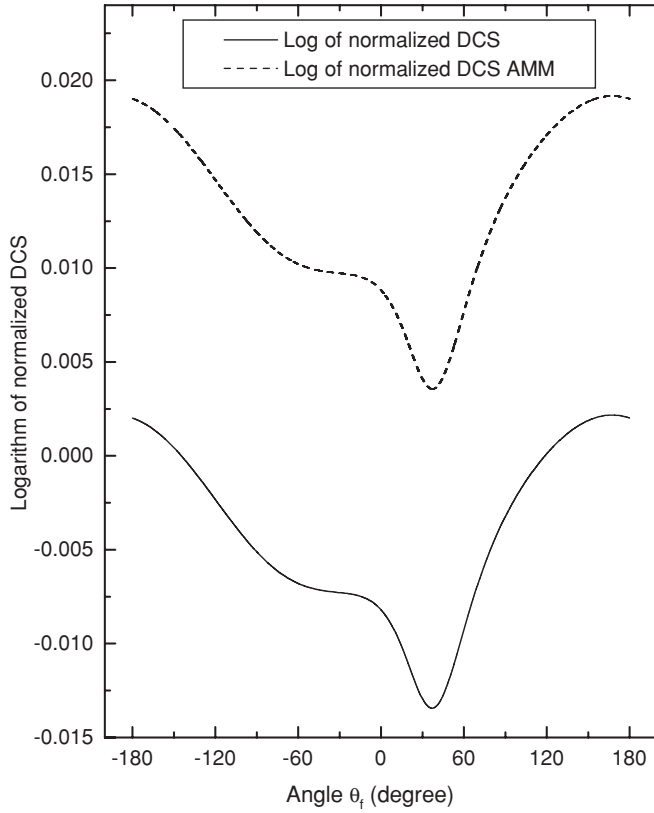


FIG. 7. Logarithm of the relativistic DCS with AMM and relativistic DCS normalized to relativistic DCS without a laser field for an electrical field strength $\varepsilon = 0.05$ a.u. and relativistic parameter $\gamma = 1.0053$. The corresponding number of photons exchanged is ± 1200 .

rule [23]: the summed DCS must always converge toward $(d\sigma/d\Omega_f)^{RNL}$ and therefore must be less than the latter. The effect of the AMM of the electron plays a key role in this behavior, but this violation has to be ascertained by increasing the number of photons. For $n = \pm 1200$ or more photons, this violation is confirmed, meaning that even at low kinetic incident energies and moderate field strength, the effect of the AMM of the electron begins to be distinguished even if this effect is small. For this number n of photons, $(d\sigma/d\Omega_f)_{AMM}^{RL}$ is higher at the peak than $(d\sigma/d\Omega_f)^{RNL}$, while $(d\sigma/d\Omega_f)^{NRL}$ and $(d\sigma/d\Omega_f)^{RL}$ are close to each other, which was to be expected since, in the nonrelativistic regime, spin effects are small. This is shown in Fig. 1. If we maintain the value of the relativistic parameter $\gamma = 1.0053$ and we increase the value of the electric field strength ε from 0.05 to 0.1 a.u., the violation of the pseudo-sum rule is still present while the difference between $(d\sigma/d\Omega_f)_{AMM}^{RL}$ and $(d\sigma/d\Omega_f)^{RL}$ is more pronounced compared to the previous case, where $\varepsilon = 0.05$ a.u. This is shown in Fig. 2, where n is also taken to have a value of ± 1200 . At the peaks of the DCSs the difference between these two is roughly equal to 6%.

As the electric field strength is increased from $\varepsilon = 0.1$ to 0.2 a.u., the physical insights mentioned are the same with a more noticeable difference between $(d\sigma/d\Omega_f)_{AMM}^{RL}$ and $(d\sigma/d\Omega_f)^{RL}$ of 36%, also at the peaks. This is shown in Fig. 3.

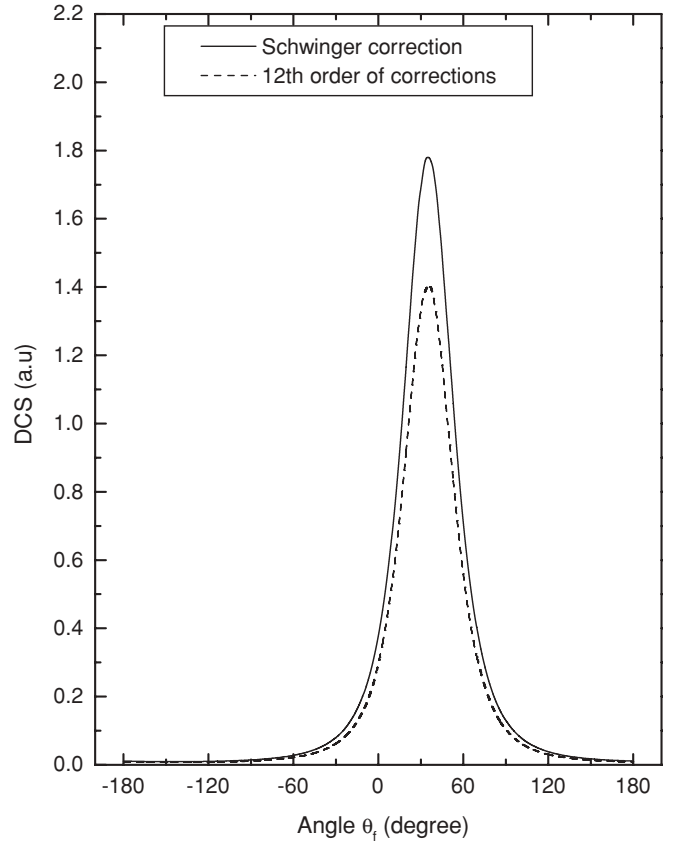


FIG. 8. Comparison between DCS with AMM for Schwinger correction and 12th order of corrections, for an electrical field strength $\varepsilon = 0.05$ a.u. and relativistic parameter $\gamma = 1.0053$. The DCSs are scaled in 10^{-3} and the corresponding number of photons exchanged is ± 1000 .

An interesting behavior (with respect to the laser angular frequency ω varying from 0.04 to 0.1 a.u. and for $n = \pm 100$ photons in the nonrelativistic regime ($\gamma = 1.0053$ and the same angular momentum coordinates) emerges with increasing ε , particularly for $\varepsilon = 0.2$ a.u., where $(d\sigma/d\Omega_f)_{AMM}^{RL}$ is similar in shape to $(d\sigma/d\Omega_f)^{RL}$ but always higher. This advocates the fact that the term $\frac{1}{2} \sum_{s_i} \sum_{s_f} |M_{fi}^{(n)}|^2$ is very sensitive to the variation of ε and this fact has to remain true for the relativistic regime. This is shown in Fig. 4.

It is then necessary to ascertain this dependence with respect to the electric field strength by varying it from $\varepsilon = 0.05$ to $\varepsilon = 1$ a.u. while retaining all these same other parameters. From $\varepsilon = 0.05$ to $\varepsilon = 0.2$ a.u., the differences between the two interesting DCSs are visible and begin to separate drastically up to $\varepsilon = 1$ a.u., where $(d\sigma/d\Omega_f)_{AMM}^{RL} \approx 11(d\sigma/d\Omega_f)^{RL}$.

Figure 5 clearly shows this behavior as well as the strong dependence with respect to the electric field strength of $(d\sigma/d\Omega_f)_{AMM}^{RL}$. Having given sound evidence of the role of the electric field strength, we now turn to the dynamical behavior of the various DCSs with respect to the relativistic parameter γ that is taken to vary from $\gamma = 1.0053$ to $\gamma = 1.025$ (i.e., maintaining the various simulations within the framework of the nonrelativistic regime). For $\varepsilon = 0.05$ a.u. and $n = \pm 200$, the difference between the two relevant DCSs is small. This is also the case for $n = \pm 400$. Moreover, increasing ε from

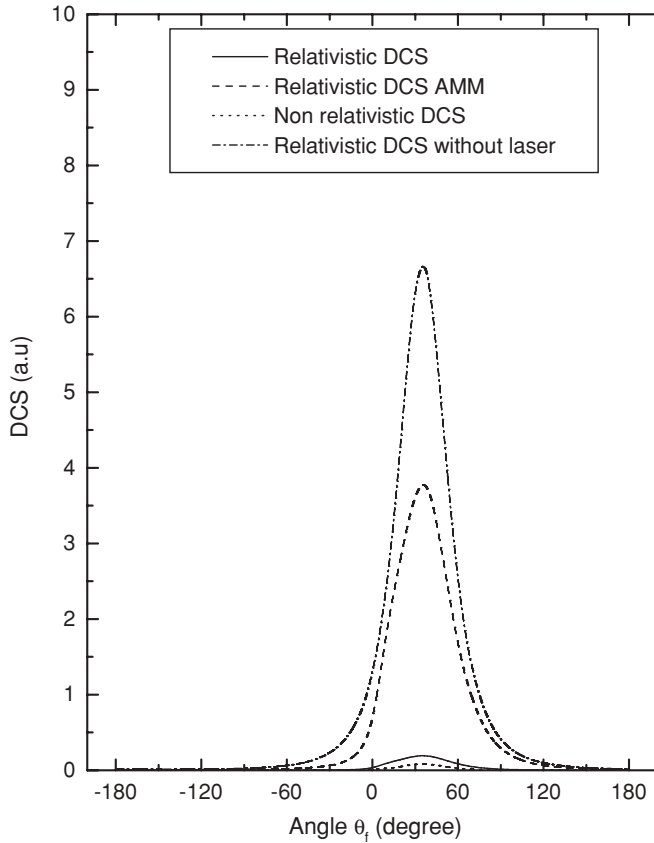


FIG. 9. The various relativistic DCSs scaled in 10^{-8} as a function of the angle θ_f in degrees for an electrical field strength of $\varepsilon = 1$ a.u. and a relativistic parameter $\gamma = 2$. The corresponding number of photons exchanged is ± 5000 .

0.05 to 0.1 a.u. and fixing n to vary between ± 1000 gives a noticeable difference between the two commonly studied DCSs while confirming the violation of the pseudo-sum rule. This is shown in Fig. 6.

Two interesting comparisons can provide further physical insights concerning this process. The first one concerns the ratios

$$R_1 = \ln \left[\left(\frac{d\sigma}{d\Omega_f} \right)_{AMM}^{RL} / \left(\frac{d\sigma}{d\Omega_f} \right)^{RNL} \right] \quad \text{and}$$

$$R_2 = \ln \left[\left(\frac{d\sigma}{d\Omega_f} \right)^{RL} / \left(\frac{d\sigma}{d\Omega_f} \right)^{RNL} \right].$$

Maintaining the same geometry and the same values of ε and γ (i.e., $\varepsilon = 0.05$ a.u. and $\gamma = 1.0053$), the upper curve for R_1 shows a minimum at the peak $\theta_f \approx 33^\circ$ and is neatly distinguishable from the second curve given by R_2 . The fact that these two curves have their minima located at $\theta_f \approx 33^\circ$ is not surprising since they have been divided by $(d\sigma/d\Omega_f)^{RNL}$ (i.e., the relativistic DCS without a laser field). Since we have taken the logarithm of the ratio of both DCSs with and without AMM, the violation of the pseudo-sum rule is clearly visible in Fig. 7, namely for R_2 . The behavior of both ratios is nearly the same as for the negative values of θ_f , meaning that, for those angles, the contribution of the term $\frac{1}{2} \sum_{s_i} \sum_{s_f} |M_{fi}^{(n)}|^2$ has an overall effect of increasing R_1 compared to that of R_2

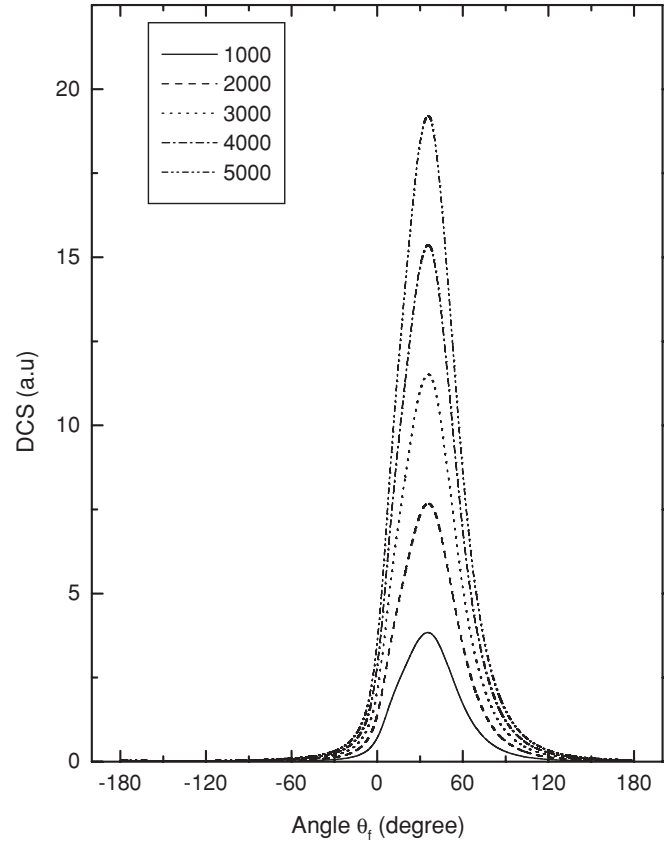


FIG. 10. The relativistic DCS with a laser field scaled in 10^{-10} for various values of number of photons exchanged, as a function of the angle θ_f in degrees for an electrical field strength of $\varepsilon = 1$ a.u. and a relativistic parameter $\gamma = 2$.

but the signature of the electron's AMM is not important. Such a behavior must be checked for the relativistic regime. Figure 7 gives the ratios R_1 and R_2 .

To end this section concerning the nonrelativistic regime, one may ask whether the value used throughout this work for the electron's anomaly is really sensitive to the order of the radiative corrections. This is indeed the case, since Fig. 8 shows that when using only the second-order radiative correction found by Schwinger [2], we have an overestimation for $(d\sigma/d\Omega_f)_{AMM}^{RL}$ (Schwinger) of about 28% compared to $(d\sigma/d\Omega_f)_{AMM}^{RL}$ (12th order), meaning that radiative corrections reduce the values of the angular distributions. We have checked this for the same geometry and for $n = \pm 1000$ photons. Needless to say, such a comparison is out of our reach in the relativistic domain since the number n must be very high to provide with a convincing conclusion.

B. The relativistic regime

The main difficulty when investigating the relativistic domain is the limitation due to available computing power (namely, an intel (R) Core (TM) 2 DUO CPU 2.2 GHz). Indeed, with such a material, it is not possible to go beyond a certain limit for n , the number of photons exchanged. We have tried, whenever possible, to extract qualitative results that do not change drastically when n is increased.

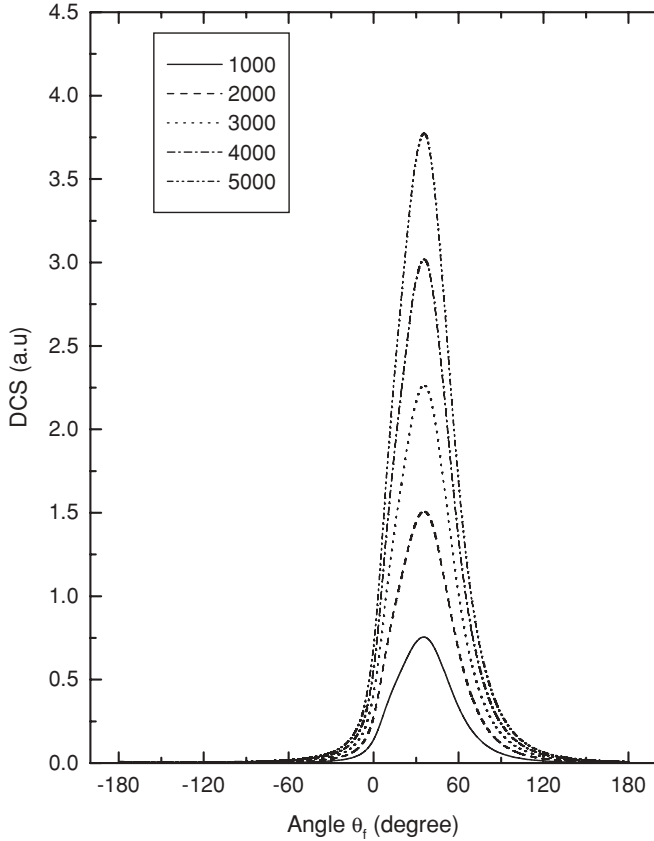


FIG. 11. The relativistic DCS with AMM scaled in 10^{-8} for various values of number of photons exchanged, as a function of the angle θ_f in degrees for an electrical field strength of $\varepsilon = 1$ a.u. and a relativistic parameter $\gamma = 2$.

The angular parameters are the same as well as the laser frequency, whereas $\varepsilon = 1$ a.u. and $\gamma = 2$.

The first physical quantities to be investigated are of course the various DCSs. Bearing in mind the limitation of our computer, we could not go beyond a certain number of photons exchanged. The first observation that can be made concerns the magnitudes of these DCSs that are strongly decreased in the relativistic regime. The dressed momentum coordinates $(\mathbf{q}_i, \mathbf{q}_f)$ are now noticeably different from the nondressed momentum coordinates $(\mathbf{p}_i, \mathbf{p}_f)$; therefore, the maximum or peak of the various DCSs is now located at nearly 29° . In this regime, the differences between $(d\sigma/d\Omega_f)^{RL}_{AMM}$ and $(d\sigma/d\Omega_f)^{RL}$ are much more pronounced than those in the nonrelativistic regime and this was to be expected because there is a strong correlation between the electric field strength and the electron's anomaly κ . Since the former is increased from $\varepsilon = 0.05$ to $\varepsilon = 1$ a.u., the dependence of the DCSs are clearly shown in Fig. 9. Figure 9 also shows that the overall behavior of $(d\sigma/d\Omega_f)^{RL}_{AMM}$ versus $(d\sigma/d\Omega_f)^{RL}$ does not vary even with increasing values of n , so we have turned our investigation to another aspect of the behavior of a sole DCS with respect to the number of photons exchanged.

Figure 10 shows the increase of $(d\sigma/d\Omega_f)^{RL}$ for the different values of the summation over n ; the first summation is over $n = \pm 1000$ photons while the last one is over $n = \pm 5000$ photons. Since the relativistic DCS without laser field is nearly

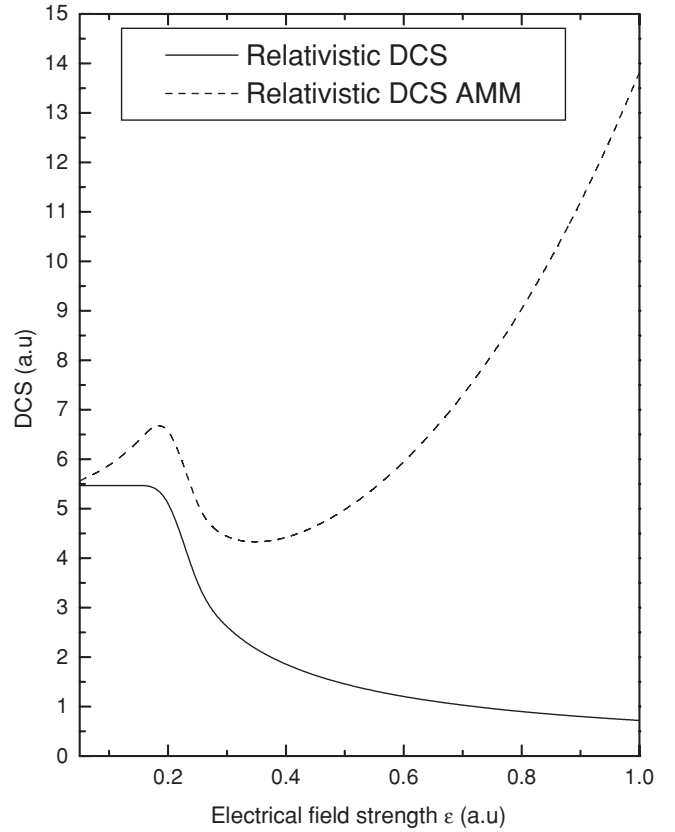


FIG. 12. The two interesting DCSs scaled in 10^{-10} as a function of electrical field strength of ε for a relativistic parameter $\gamma = 2$ and an angle $\theta_f = 135^\circ$. The corresponding number of photons exchanged is $\pm 20\,000$.

6.75×10^{-8} at its maximum, it is obvious that one has to sum over a very large number of photons exchanged in order to obtain at least the 10^{-8} order of magnitude. Even for $n = \pm 5000$, the value of $(d\sigma/d\Omega_f)^{RL}$ is nearly 2×10^{-9} at its maximum. As there is a linear relation between the summation over n and the value of $(d\sigma/d\Omega_f)^{RL}$ at its peak, however, it is possible to investigate this dependence by reducing the angular distribution interval.

In Fig. 11, we show the same dependence of $(d\sigma/d\Omega_f)^{RL}_{AMM}$ and what emerges is a very different picture. Indeed, the value of this DCS at its maximum is now 4×10^{-8} for $n = \pm 5000$, which is close to the value of $(d\sigma/d\Omega_f)^{RL}$ at the same maximum. This means that, by reducing the angular distribution interval, we can investigate if there is violation of the pseudo-sum rule as in the nonrelativistic regime. An interesting behavior emerges when we vary the electrical field strength from $\varepsilon = 0.05$ to $\varepsilon = 1$ a.u. As $\gamma = 2$, there is an interval of values (0.05, 0.19) where there is a very weak quasilinear decrease of $(d\sigma/d\Omega_f)^{RL}$ and this DCS decrease occurs in a more pronounced manner in the interval (0.2, 0.3) while smoothly decreasing for other values of ε . This is consistent with the results shown in Figs. 10 and 11, where the various DCSs have decreased values for $\gamma = 2$ and $\varepsilon = 1$ a.u. As for the quasilinear decrease of $(d\sigma/d\Omega_f)^{RL}$, the explanation is rather obvious since these values of ε are in the vicinity of a “quasi-non-relativistic” regime as long as we consider only ε . Indeed, considering the summation

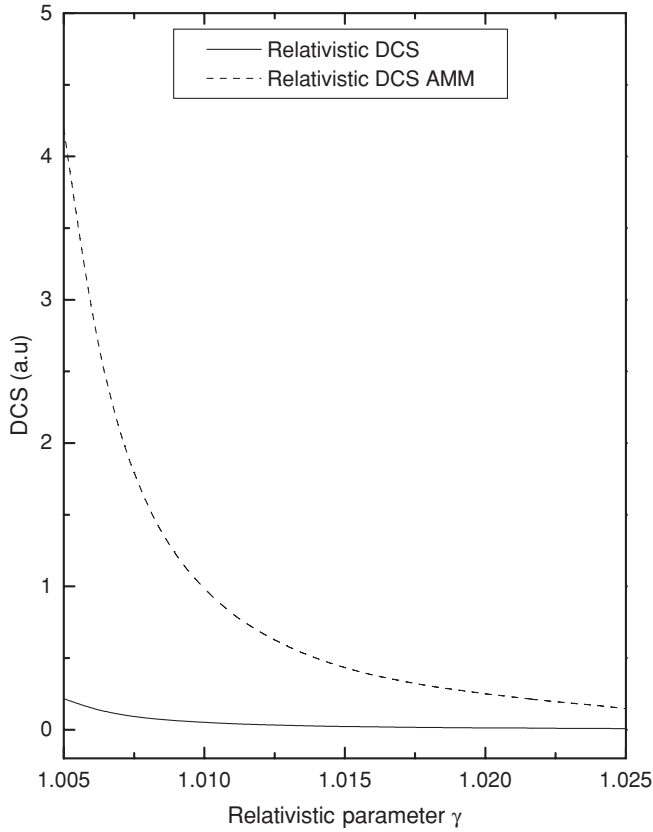


FIG. 13. Various DCSs scaled in 10^{-4} as a function of relativistic parameter γ for an electrical field strength of $\varepsilon = 1$ a.u. and an angle $\theta_f = 135^\circ$. The corresponding number of photons exchanged is $\pm 10\,000$.

over n ($\pm 20\,000$), this plateau-like behavior means that we have reached and overtaken the required summation over n for which $(d\sigma/d\Omega_f)^{RL}$ converge to $(d\sigma/d\Omega_f)^{RNL}$.

A contrasting behavior is observed for $(d\sigma/d\Omega_f)_{AMM}^{RL}$, where we have summed over $\pm 20\,000$ photons, as before. Even for $\gamma = 2$, both DCSs remain close for small values of ε (typically 0.05, 0.075) but begin to deviate from each other as ε increases. A peak of $(d\sigma/d\Omega_f)_{AMM}^{RL}$ is present for $\varepsilon \simeq 0.19$ a.u., and then there is a minimum for $\varepsilon \simeq 0.38$ a.u. and then a rapid increase for greater values of ε . The latter can be easily explained since the spinor part of $(d\sigma/d\Omega_f)_{AMM}^{RL}$ is strongly dependent on both ε and κ . The first maximum and the next minimum are difficult to interpret since the expression of $\frac{1}{2} \sum_{s_i} \sum_{s_f} |M_{fi}^{(n)}|^2$ is very long and not prone to analytical investigation. However, since the angular parameters are fixed ($\gamma = 2$), these can only be tracked back to the overall dependence of the spinor part of $(d\sigma/d\Omega_f)_{AMM}^{RL}$ on the electric field strength. These dependencies with respect to ε for both DCSs are shown in Fig. 12.

The relativistic effects on these DCSs can be investigated by varying the relativistic parameter γ . The number of photons exchanged is $\pm 10\,000$. But as we have $\varepsilon = 1$ a.u., the interpretation of the curve obtained when γ starts from 1.005 and increases to a value of 1.025 must be cautiously carried out since there is an interplay between relativistic effect due to the variation of γ and the fixed value of ε ,

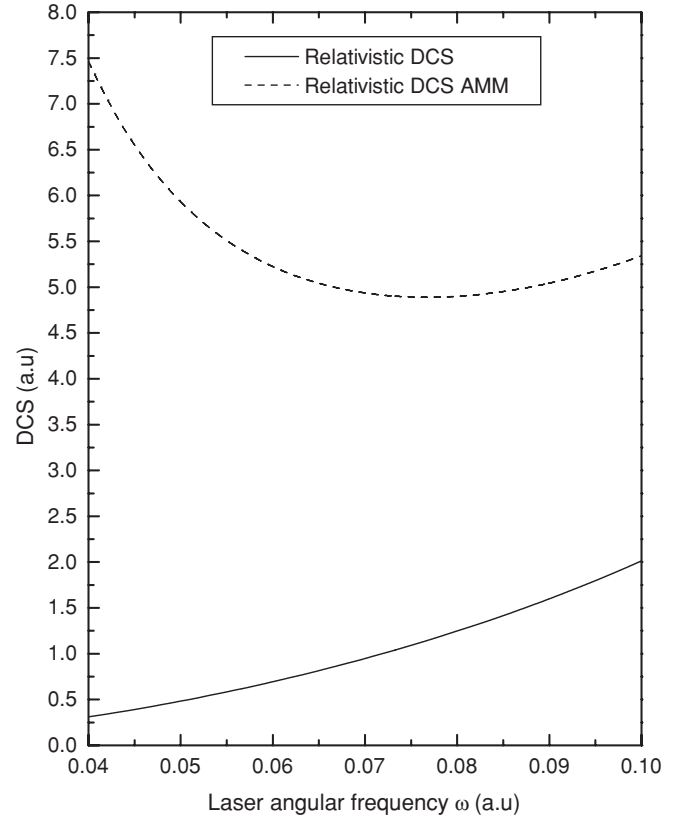


FIG. 14. The various relativistic DCSs scaled in 10^{-10} as a function of ω for an electrical field strength of $\varepsilon = 1$ a.u., a relativistic parameter $\gamma = 2$, and an angle $\theta_f = 135^\circ$. The corresponding number of photons exchanged is $\pm 10\,000$.

on the one hand, while it does not give the whole picture of what really happens when γ varies from 1.005 to 2, on the other hand. We have remedied this computational task by studying three regions for the variation of γ , namely (1.005, 1.025), (1.495, 1.505), and (1.995, 2). An additional difficulty arises when varying γ (while ε remains fixed, $\varepsilon = 1$ a.u.), because both DCSs decrease by a factor of magnitude 4 (from $\sim 10^{-4}$ to 10^{-8}) when γ approaches 2. Therefore, even if $(d\sigma/d\Omega_f)_{AMM}^{RL}$ is always greater than $(d\sigma/d\Omega_f)^{RL}$, this cannot be visually translated in Fig. 13. However, simulations for $\gamma \in (1.495, 1.505)$ and $\gamma \in (1.995, 2)$ give results that are consistent with previous results. The effect of the frequency ω is shown in Fig. 14 by varying ω from 0.04 to 0.1 a.u., for a relativistic parameter $\gamma = 2$, an electric field strength $\varepsilon = 1$, and for $n = \pm 10\,000$ photons. In this regime, the DCSs are not similar in shape, as in the nonrelativistic regime (see Fig. 4). While both DCSs decrease in value (by an order of magnitude 3), $(d\sigma/d\Omega_f)^{RL}$ is roughly quasilinear, whereas $(d\sigma/d\Omega_f)_{AMM}^{RL}$ decreases from its maximum value 7.5×10^{-10} (a.u.) to a minimum located at 5×10^{-10} (a.u.) and then increases.

IV. CONCLUSION

In this work, we have presented results concerning the effects of the electron's anomalous magnetic moment on the process of laser-assisted electron-atomic hydrogen elastic

collisions. Throughout this work we have used the recent experimental value of the anomaly a found by Gabrielse [3]. We have focused our study on the electronic dressing with the addition of the electron anomaly. Using the Dirac-Volkov wave function that incorporates this anomaly [18], we found the analytical expression of the corresponding DCS. A spatial integral part that was found in a previous work [21] remains the same for the study of this process. The various coefficients that intervene in the expression of S_{fi} have been obtained using REDUCE [22]. We have the same formal analogy between the DCS without and with anomaly. However, the spinor part incorporating the latter condition is strongly dependent

on the electron's anomaly and on the electric field strength. For the nonrelativistic regime, the addition of the electron's AMM is noticeable but small. When increasing the electric field strength to moderate values, this effect becomes more pronounced. We have obtained the violation of the pseudo-sum rule [23]. We have also checked that the second-order correction due to Schwinger [2] overestimates the DCS. In the relativistic regime, the dynamical behavior of the DCS shows that the correlation between the terms stemming from the electron's anomaly and the electric field strength is more pronounced even if there is an overall decrease of DCS without the electron's anomaly and the DCS with the electron's anomaly.

-
- [1] M. E. Peskin and D. V. Schroeder, *An Introduction to Quantum Field Theory* (Perseus Books Publishing, Reading, MA, 1995).
- [2] J. Schwinger, *Phys. Rev.* **73**, 416 (1948).
- [3] D. Hanneke, S. Fogwell, and G. Gabrielse, *Phys. Rev. Lett.* **100**, 120801 (2008).
- [4] E. Remiddi, *Status of QED Prediction of g-2*, PhiPsi08, International Workshop on e+e-collisions from Phi to Psi (Laboratori Nazionale di Frascati, Italy, April 2008).
- [5] D. M. Volkov, *Z. Phys.* **94**, 250 (1935).
- [6] J. San Roman, L. Plaja, and L. Roso, *Phys. Rev. A* **64**, 063402 (2001).
- [7] L. S. Brown and T. W. B. Kibble, *Phys. Rev.* **133**, A705 (1964).
- [8] O. von Roos, *Phys. Rev.* **135**, A43 (1964).
- [9] Z. Fried and J. H. Eberly, *Phys. Rev.* **136**, B871 (1964).
- [10] T. W. B. Kibble, *Phys. Rev.* **150**, 1060 (1966).
- [11] E. S. Sarachik and G. T. Schappert, *Phys. Rev. D* **1**, 2738 (1970).
- [12] H. R. Reiss, *Opt. Express* **2**, 261 (1998).
- [13] *Strong Field Laser Physics*, edited by T. Brabec, Springer Series in Optical Sciences (Springer, Berlin, 2008).
- [14] E. Lötstedt, Ph.D. thesis, University of Heidelberg, Germany, 2008.
- [15] E. Lötstedt, U. D. Jentschura, and C. H. Keitel, *Phys. Rev. Lett.* **98**, 043002 (2007).
- [16] S. Schnez, E. Lötstedt, U. D. Jentschura, and C. H. Keitel, *Phys. Rev. A* **75**, 053412 (2007).
- [17] J. D. Bjorken and S. D. Drell, *Relativistic Quantum Mechanics* (McGraw-Hill, New York, 1964).
- [18] Y. I. Salamin, *J. Phys. A* **26**, 6067 (1993).
- [19] J. M. Djiokap, H. M. Tetchou Nganso, and M. G. Kwato Njock, *Phys. Scr.* **75** 726 (2007).
- [20] W. Greiner and J. Reinhardt, *Quantum Electrodynamics*, 3rd ed. (Springer, Berlin, 2003).
- [21] Y. Attaourti, B. Manaut, and A. Makhoute, *Phys. Rev. A* **69**, 063407 (2004).
- [22] A. G. Grozin, *Using REDUCE in High Energy Physics* (Cambridge University, Cambridge, England, 1997).
- [23] N. M. Kroll and K. M. Watson, *Phys. Rev. A* **8**, 804 (1973).